



1 Article

2 Differential Study of Projectile Coherence Effects on

3 Double Capture Processes in p + Ar Collisions

- Trevor Voss 1,2, Basu R. Lamichhane 1,3 Madhav Dhital 1, Ramaz Lomsadze 4, and Michael Schulz 5 1,*
- Department of Physics and LAMOR, Missouri University of Science & Technology, Rolla, MO 65409, USA; tvoss15@gmail.com (T.V.); tud10959@temple.edu (B.R.L.); md8rd@mst.edu (M.D.)
- 8 ² Biophotonics Center, Vanderbilt University, Nashville, TN 37235, USA
- 9 ³ Physics Dept., Temple University, Philadelphia, PA 19122, USA
- 10 4 Tbilisi State University, Tbilisi 0179, Georgia; lomsadze86@hotmail.com
- * Correspondence: schulz@mst.edu
- Received: 15 February 2020; Accepted: date; Published: date
- Abstract: We have measured differential yields for double capture and double capture accompanied
- by ionization in 75 keV p + Ar collisions. Data were taken for two different transverse projectile coherence lengths. A small effect of the projectile coherence properties on the yields were found
- 15 coherence lengths. A small effect of the projectile coherence properties on the yields were found 16 for double capture, but not for double capture plus ionization. The results suggest that multiple
- projectile target interactions can lead to a significant weakening of projectile coherence effects.
- 18 **Keywords:** ion-atom collisions; few-body problem; coherence effects; charge exchange

19 _

20

21

22

23

24

25

26

27

28

29

30

31

32

33

34

35

36

37

38

39

40

41

42

43

1. Introduction

Studies of atomic collisions are particularly suitable to study the fundamentally important few-body problem (FBP) [1,2]. The essence of the FBP is that the Schrödinger equation is not analytically solvable for more than two mutually interacting particles even when the forces acting within the system under investigation are precisely known. Theory therefore has to resort to heavy modelling efforts and the assumptions and approximations entering in these models have to be tested by detailed experimental data.

In most cases, the quantity that is measured in a collision experiment is the cross section for a specific process selected in the experiment. In the case of heavy projectile collisions, these cross sections are theoretically often treated within perturbative models [e.g.,3]. For electron impact, non-perturbative methods are routinely applied [e.g.,4–6], however, for ion impact such approaches [e.g. 7–10] are much more challenging and still relatively rare compared to perturbative calculations. One well-established perturbative model is represented by the Born series. There, the target is described by eigenstates of the unperturbed target Hamiltonian and the projectile by plane waves. The transition amplitude is then expanded in powers of the interaction potential.

Some of the limitations of the Born series in accurately describing processes occurring in atomic collisions are well known [e.g.,3]. For example, it represents a two-state approximation because it considers only one target eigenstate for the incoming channel (typically the ground state) and one in the outgoing channel. As a result, couplings between different eigenstates in the final state, which can be very important especially at small collision velocities, are completely ignored. Furthermore, in practice, the power series has to be truncated after some term and to the best of our knowledge no calculations beyond second order have been published yet [e.g.,11–13]. Some of these shortcomings are circumvented in distorted wave approaches [e.g.,14–16]. However, recently, we demonstrated that in ionization of H₂ and He by intermediate energy proton impact even distorted wave

calculations do not give satisfactory results if the electron is ejected with a velocity close to the projectile velocity [17,18].

Another shortcoming of the Born series (and other methods including non-perturbative approaches) did not receive much attention until about a decade ago [19]. It results from the description of the incoming projectile in terms of a plane wave, which implies that the projectile has a sharp momentum. However, in reality the projectiles have an intrinsic momentum distribution of finite width. This means that the projectiles are not fully coherent and, in some cases (depending on the dimension of the diffracting object) may even be largely incoherent. As a result, interference effects predicted by theory are not always experimentally observable. Indeed, in the scattering angle dependence of measured double differential ionization cross section for $p + H_2$ collisions, interference structures were observed for a coherent projectile beam, but were absent for an incoherent beam [19]. In numerous follow-up experiments, similar projectile coherence effects on the cross sections were observed [20–30] (for a review see [31]). Furthermore, the interpretation of the experimental data was supported by several theoretical studies [e.g.,32–36].

In measured fully differential cross sections (FDCS) for dissociative capture leading to relatively large kinetic energy releases (KER) in $p + H_2$ collisions [28] such projectile coherence effects were found to be less pronounced than in single ionization or capture. In the case of Coulomb explosion following double capture, such effects were not discernable at all [28]. This was interpreted as a "washing out" of the phase due to multiple projectile scatterings leading to dissociative capture. For large KER values dissociative capture proceeds predominantly through excitation of the second target electron. At the relatively small projectile energy of 75 keV the capture and excitation occur mostly through two independent interactions of the projectile with each electron. Therefore, the final scattering angle observed in the experiment is due to a convolution of two scattering angles from these two interactions. The phase depends on the scattering angle in each interaction and is thus no longer unambiguously determined by the measured total scattering angle.

One complication in this interpretation is that the experiment used a diatomic molecular target. As a result, both single- and two-center interference can contribute to the cross sections measured for a coherent beam [24]. In the former, different paths (impact parameters) leading to the same scattering angle and in the latter waves diffracted from the two centers of the molecule interfere with each other. For both types of interference the phases may differ from each other, which can also contribute to a "washing out" of any interference structure. Therefore, to trace the reasons for the (near) absence of coherence effects in double capture it is important to perform the experiment for an atomic target. Differential double capture cross sections have been measured for $He^{2+} + He [37–39]$ and for p + He collisions [40]. However, all of these experiments were performed for only one projectile coherence length.

In this article, we present measured differential cross sections for double capture (DC) and for double capture plus single ionization (DCI) for 75 keV p + Ar collisions. Data were taken for two different coherence lengths and the interference term was extracted by analyzing the ratios between the cross sections for the larger and smaller coherence length. The data reveal less pronounced coherence effects than observed previously for single ionization [19] or single capture [20], but a more pronounced effects than in DC from a molecular target [28]. Furthermore, we analyzed the ratios between the DCI and DC cross sections and found some similarities to transfer-ionization to single capture cross section ratios measured earlier [41].

2. Experiment

The experiment was performed in the accelerator laboratory at the Missouri University of Science & Technology. Protons generated with a hot cathode ion source were accelerated to 75 keV. The beam was collimated with a pair of slits with a width of 150 μ m. The horizontal slit, defining scattering in the y-direction, was placed at a distance of 50 cm from the target, and the vertical slit at a distance of 6.5 cm. The coherence length is determined by the slit geometry through the relation.

$$\Delta r = L\lambda/2a \tag{1}$$

Where L is the distance of the slit to the target, a is the width of the slit, and λ is the deBroglie wavelength of the projectiles [31]. In the y- and x-directions, this relation yields coherence lengths of 3.3 a.u. and 0.4 a.u., respectively [31]. However, in the x-direction the local collimation angle (which is determined by a/L in equation 1) is not limited by the collimating slit, but rather by an aperture in the accelerator terminal. As a result, the actual coherence length in the x-direction is nearly 1 a.u. Scattered projectiles with a negative charge were selected by a switching magnet and recorded by a two-dimensional position-sensitive multi-channel plate detector. In the data analysis, scattering of coherent and incoherent projectiles was selected by setting conditions on the projectile position spectrum corresponding to scattering in the y- and x-directions, respectively.

The incoming projectile beam was crossed with a very cold neutral Ar beam from a supersonic gas jet. Positively charged recoil ions were extracted by a weak electric field of 6 V/cm, drifted in a field-free region, and were recorded by a second position-sensitive multi-channel plate detector. This set-up in general is used to measure the momentum of the recoil ions. However, due to the large target mass the momentum resolution is significantly worse than for He or H_2 targets. Therefore, we did not use the momentum information and as a result, the initial state from which electrons are captured was not determined. In contrast, the final state of the captured electrons is fully determined because there is only one bound state in H_2 .

The projectile and recoil-ion detectors were set in coincidence. Since the time of flight of the recoil ions from the collision region to the detector depends on $\sqrt{M/q}$ (where M/q is the mass to charge ratio of the recoil ion), q could be determined in the coincidence time spectrum. Coincidences with q=2 reflect DC and coincidences with q=3 DCI. From the projectile position information the scattering θ_P was obtained. Therefore, the θ_P -dependence of the cross sections differential in the projectile solid angle was extracted from the data. However, since no normalized total double capture cross sections are available for p+Ar, the cross section could not be put on an absolute scale.

3. Results and Discussion

In Figure 1 the differential yield (i.e., the unnormalized differential cross section) for DC is plotted as a function of θ_P . The closed symbols represent data for projectile scattering in the y-direction, to which we refer as the coherent data, and the open symbols projectile scattering in the x-direction (incoherent data). It should be noted that the term "coherent" is relative as it refers to the coherence length relative to the effective dimension of the diffracting object. With regard to single-center interference the effective target dimension is given by the impact parameter range which significantly contributes to the process under investigation. Although this range is not a well-known quantity, in the case of DC it is clear that the process is dominated by impact parameters significantly smaller than 3.3 a.u. (where 1 a.u. is the Bohr radius of the H-atom for n=1), which is considerably larger than the size of the neutral Ar atom of 2 a.u. It is therefore justified to consider the data for projectile scattering in the y-direction as coherent. On the other hand, it is not so clear how important impact parameters around 1 a.u. are in DC. We nevertheless refer to the data for projectile scattering in the x-direction as incoherent because any interference which may be found in measured data should be less pronounced for the smaller coherence length.

The shapes of the θ_P -dependence of the differential cross sections look very similar. Nevertheless, there are small, but significant differences. At the smallest θ_P the coherent data are slightly below and between 2 and 3 mrad above the incoherent data. It should be noted that up to about 3 mrad the statistical error bars are smaller than the size of the data points.

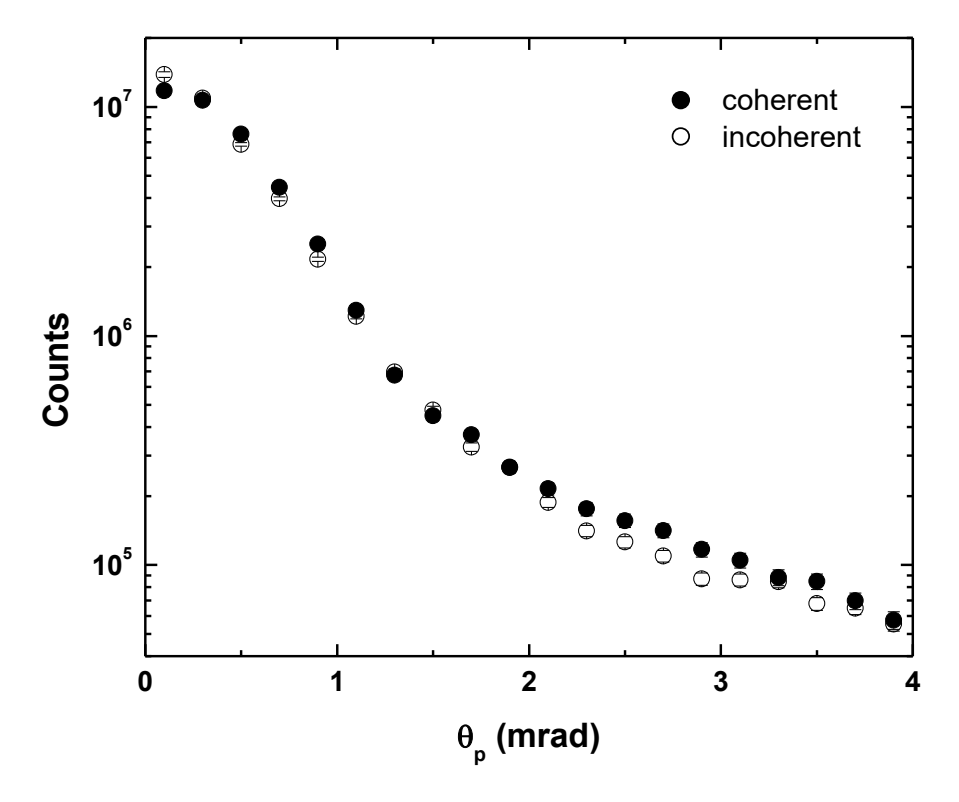


Figure 1. Differential yield (counts) for double capture in 75 keV p + Ar collisions as a function of projectile scattering angle. The closed symbols represent data taken for the larger projectile coherence length and the open symbols those taken for the smaller coherence length.

Due to the steep dependence of the data on θ_P and the logarithmic scale on the vertical axis, the differences between the coherent and incoherent data sets may appear less pronounced than they are. A clearer picture emerges by analyzing the ratios RDC between both data sets as a function of θ_P . These ratios, which qualitatively represent the interference term, are plotted in Figure 2. A small-amplitude oscillatory structure can be seen, reflecting weak coherence effects. In the case of single ionization a simple model single-center interference term was suggested as [22,23]

$$I_s = 1 + \alpha \cos(q_{tr} \Delta b) \tag{2}$$

Where q_{tr} = $p_0 \sin(\theta_P)$ is the transverse component of the momentum transfer ${\bf q}$ and Δb is an effective range of impact parameters reflecting the effective target dimension. α describes the damping of the oscillation due to the finite or non-zero coherence length for the coherent and incoherent data, respectively.

A best fit of I_s to R_{DC}, shown as the solid curve in Figure 2, yields $\alpha = 0.15 \pm 0.05$ and $\Delta b = 0.7 \pm 0.03$ a.u. Except for $\theta_P < 0.5$ mrad this model interference term reproduces the experimental data reasonably well. The disagreement at small θ_P probably reflects the limitation of the simple model interference term of equation (2). For single ionization the same fitting routine yielded parameters of $\alpha = 0.3$ to 0.7 and $\Delta b = 1.4$ to 2 a.u. (depending on target and ejected electron energy). The significantly smaller effective target dimension in DC is expected, as this process requires, on average, much closer collisions than single ionization. The much smaller value of α shows that here projectile coherence effects are much less pronounced. However, they are nevertheless more pronounced than in DC from H₂, where they are essentially completely absent [28]. This suggests that indeed the phase is not unambiguously determined by the measured scattering angle due to multiple projectile scattering in two-electron processes (as argued in [28]). For a molecular target, the single-center interference structure is further "washed out" by the presence of two-center interference.

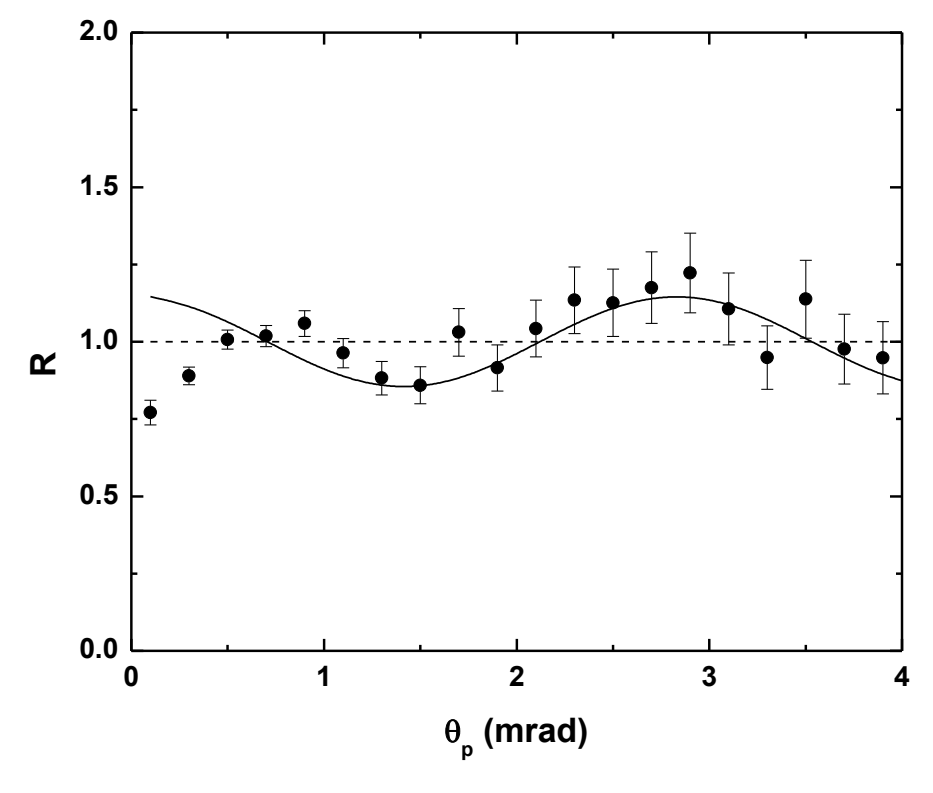


Figure 2. Ratios RDC between the coherent and incoherent yields of Figure 1 as a function of scattering angle. The curve shows a best fit of equation (1) to the measured ratios.

In Figure 3 the differential yield for DCI is plotted as a function of θ_P , where again the closed symbols represent the coherent and the open symbols the incoherent data. These angular distributions fall off slower with increasing θ_P compared to their counterparts for DC. More specifically, the angle at which the yield is reduced by a factor of 2 compared to $\theta_P = 0$ is larger by about 20% than in the case of DC. This is not surprising considering that DCI is a three-electron process requiring even closer collisions than DC. No differences of statistical significance between the coherent and incoherent data can be discerned. The ratios between the coherent and incoherent yields, plotted in Figure 4, do not give a clear answer either: at small θ_P the ratios seem to be somewhat smaller than 1 (signifying destructive interference). However, for $\theta_P > 1.5$ mrad the data are consistent with RDCI = 1 and as a result, the oscillatory structure seen in the ratios for DC cannot be clearly identified for DCI. This could at least partly be due to the larger statistical error bars. On the other hand, a less pronounced interference structure is consistent with the notion that multiple projectile scattering can "wash out" the phase information, which for a single interaction is contained in the measured scattering angle.

179

180

181

182

183

184

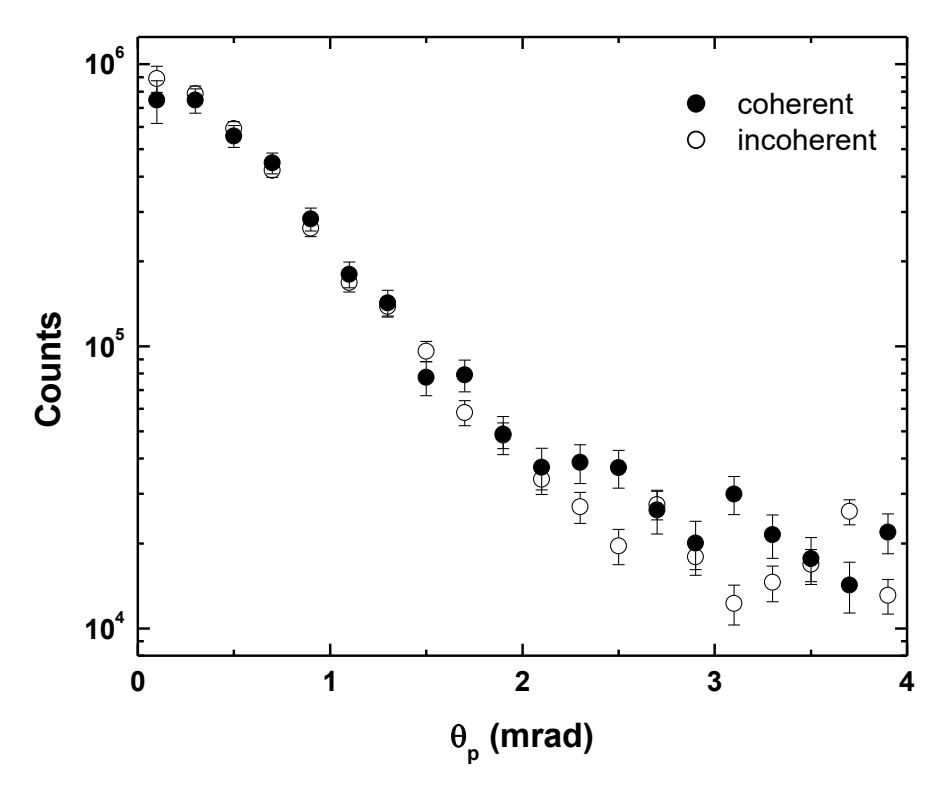


Figure 3. Same as Figure 1, but for double capture plus single ionization.

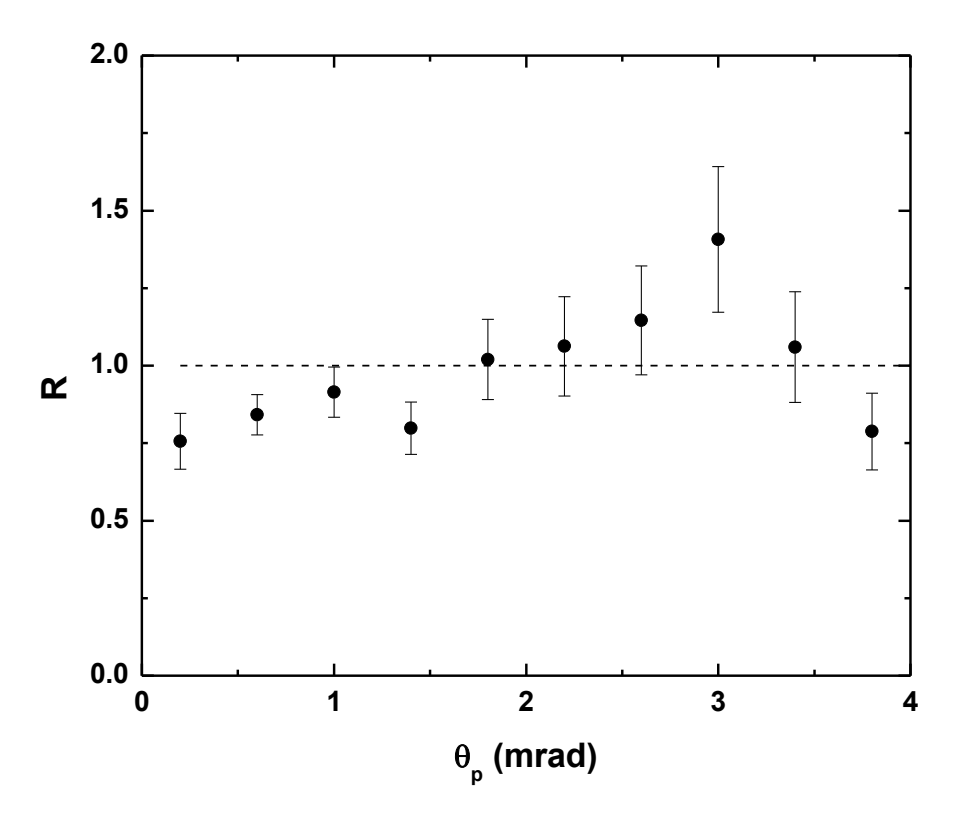


Figure 4. Same as Figure 2, but for double capture plus single ionization.

Finally, we analyzed the ratios between the DCI and DC yields as a function of θ_P , which are plotted in Figure 5 for coherent (closed symbols) and incoherent (open symbols) projectiles. In an independent electron model, these ratios reflect the single ionization probability $P(\theta_P)$. The same

191192

193

194

195

196

197

198

199

200

201

202

203

204

205

206

207

208

209

210

211

212

213

185

probability can also be obtained as the ratio between e.g., transfer-ionization and single capture cross sections, which were measured by Bross et al. [41] for 50 to 175 keV p + He collisions. Indeed, these data closely resemble the θ_P -dependence of the ratios measured in the present study: in both cases R steeply rises between 1 and 1.5 mrad to reach a plateau at $\theta_P > 1.5$ mrad. However, the p + Ar data are significantly larger in magnitude, which is due to the larger number of electrons in the valence shell of Ar compared to He. No differences between the coherent and incoherent data are found.

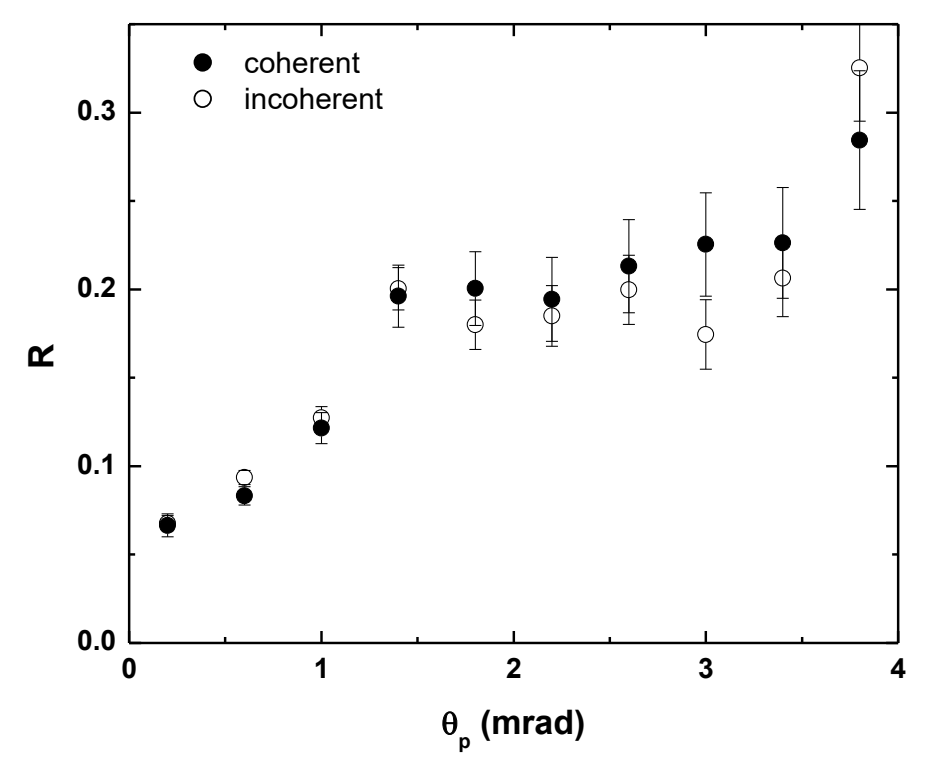


Figure 5. Ratios RDCI/DC between the double capture plus ionization and the pure double capture yields as a function of scattering angle. Symbols as in Figs. 1 and 3.

4. Conclusions

We have performed an experimental differential study on double capture processes in p + Ar collisions. The projectile scattering angle distributions of the reaction yield were measured for two different coherence lengths and the interference term was extracted as the ratio between these yields. Data were obtained for pure double capture and for double capture accompanied by ejection of a third target electron. In the case of pure double capture a weak structure was observed in the interference term, signifying projectile coherence effects. These effects were less pronounced than in previous data obtained for one-electron processes (ionization or capture), but more pronounced than in double capture from H₂. These observations suggest that multiple projectile interactions in two-(or three-) electron processes soften the relation between the phase angle and the measured total projectile scattering angle. Furthermore, the comparison to previously taken data for double capture from H₂ suggest that there the presence of two-center interference further "blurs" the single-center interference structure. In the case of double capture plus ionization from Ar no significant projectile coherence effects were found. This could partly be due to the lower statistics (compared to pure double capture). However, the fact that the projectile has to undergo an additional interaction (if correlated processes are ignored) could also contribute to the weakening of projectile coherence effects.

Acknowledgements

The financial support from the National Science Foundation under grant no. PHY-1703109 is gratefully acknowledged.

214 References

- 215 1. M. Schulz, R. Moshammer, D. Fischer, H. Kollmus, D.H. Madison, S. Jones, and J. Ullrich, Nature 422, 48 (2003)
- 2. M. Schulz and D.H. Madison, International Journal of Modern Physics A 21, 3649 (2006)
- 218 3. J.R. Taylor, Scattering Theory: The Quantum Theory of Nonrelativistic Collisions (Wiley, New York, 1972)
- 219 4. T. Rescigno, M. Baertschy, W.A. Isaacs, and C.E. McCurdy, Science 286, 2474 (1999)
- X. Ren, I. Bray, D.V. Fursa, J. Colgan, M.S. Pindzola, T. Pflüger, A. Senftleben, S. Xu, A. Dorn, and J. Ullrich,
 Phys. Rev. A 83, 052711 (2011)
- 222 6. J. Colgan, M. Foster, M.S. Pindzola, I. Bray, A.T. Stelbovis, and D.V. Fursa, J. Phys. B 42, 145002 (2009)
- 223 7. M. McGovern, C.T. Whelan, and H.R.J. Walters, Phys. Rev. A 82, 032702 (2010)
- 224 8. M.F. Ciappina, M.S. Pindzola, and J. Colgan, Phys. Rev. A 87, 042706 (2013)
- 225 9. I.B. Abdurakhmanov, J.J. Bailey, A.S. Kadyrov, and I. Bray, Phys. Rev. A 97, 032707 (2018)
- 226 10. M. Baxter, T. Kirchner, and E. Engel, Phys. Rev. A 96, 032708 (2017)
- 227 11. J. H. McGuire and J. Eichler, Phys. Rev. A 28, 2104 (1983)
- 228 12. A.B. Voitkiv, B. Najjari, and J. Ullrich, J. Phys. B 36, 2591 (2003)
- O. Chuluunbaatar, S.A. Zaytsev, K.A. Kouzakov, A. Galstyan, V.L. Shablov, and Yu.V. Popov, Phys. Rev.
 A 96, 042716 (2017)
- 14. D. H. Madison, D. Fischer, M. Foster, M. Schulz, R. Moshammer, S. Jones, and J. Ullrich, Phys. Rev. Lett.
 91, 253201 (2003)
- 233 15. R.T. Pedlow, S.F.C. O'Rourke, and D.S.F. Crothers, Phys. Rev. A 72, 062719 (2005)
- 234 16. A.B. Voitkiv, Phys. Rev. A 95, 032708 (2017)
- 235 17. M. Dhital, S. Bastola, A. Silvus, A. Hasan, B.R. Lamichhane, E. Ali, M.F. Ciappina, R.A. Lomsadze, D. Cikota, B. Boggs, D.H. Madison, and M. Schulz, Phys. Rev. A 99, 062710 (2019)
- 237 18. M. Dhital, S. Bastola, A. Silvus, B.R. Lamichhane, E. Ali, M.F. Ciappina, R. Lomsadze, A. Hasan, D.H. Madison, and M. Schulz, Phys. Rev. A 100, 032707 (2019)
- 239 19. K.N. Egodapitiya, S. Sharma, A. Hasan, A.C. Laforge, D.H. Madison, R. Moshammer, and M. Schulz, Phys. Rev. Lett. 106, 153202 (2011)
- 241 20. S. Sharma, A. Hasan, K.N. Egodapitiya, T. P. Arthanayaka, and M. Schulz, Phys. Rev. A 86, 022706 (2012)
- 242 21. K. Schneider, M. Schulz, X. Wang, A. Kelkar, M. Grieser, C. Krantz, J. Ullrich, R. Moshammer, and D. Fischer, Phys. Rev. Lett. 110, 113201 (2013)
- S. Sharma, T.P. Arthanayaka, A. Hasan, B.R. Lamichhane, J. Remolina, A. Smith, and M. Schulz, Phys. Rev.
 A 89, 052703 (2014)
- S. Sharma, T.P. Arthanayaka, A. Hasan, B.R. Lamichhane, J. Remolina, A. Smith, and M. Schulz, Phys. Rev. A 90, 052710 (2014)
- 248 24. T.P. Arthanayaka, S. Sharma, B.R. Lamichhane, A. Hasan, J. Remolina, S. Gurung, and M. Schulz, J. Phys. B 48, 071001 (2015)
- 25. T.P. Arthanayaka, S. Sharma, B.R. Lamichhane, A. Hasan, J. Remolina, S. Gurung, L. Sarkadi, and M. Schulz, J. Phys. B 48, 175204 (2015)
- 252 26. T. Arthanayaka, B.R. Lamichhane, A. Hasan, S. Gurung, J. Remolina, S. Borbély, F. Járai-Szabó, L. Nagy, and M. Schulz, J. Phys. B 49, 13LT02 (2016)
- 254 27. B.R. Lamichhane, T. Arthanayaka, J. Remolina, A. Hasan, M.F. Ciappina, F. Navarrete, R.O. Barrachina, R.A. Lomsadze, and M. Schulz, Phys. Rev. Lett. 119, 083402 (2017)
- 28. B.R. Lamichhane, A. Hasan, T. Arthanayaka, M. Dhital, K. Koirala, T. Voss, R.A. Lomsadze, and M. Schulz, Phys. Rev. A 96, 042708 (2017)
- M. Schulz, A. Hasan, B. Lamichhane, T. Arthanayaka, M. Dhital, S. Bastola, L. Nagy, S. Borbély, and F. Járai-Szabó, accepted for publication in J. Phys. Conf. Proc. (2020)
- 30. H. Gassert, O. Chuluunbaatar, M. Waitz, F. Trinter, H.-K. Kim, T. Bauer, A. Laucke, Ch. Müller, J.
 Voigtsberger, M. Weller, J. Rist, M. Pitzer, S. Zeller, T. Jahnke, L. Ph. H. Schmidt, J. B. Williams, S. A.
- Zaytsev, A. A. Bulychev, K. A. Kouzakov, H. Schmidt-Böcking, R. Dörner, Yu. V. Popov, and M. S. Schöffler, Phys. Rev. Lett. 116, 073201 (2016)
- 264 31. M. Schulz, Ad. At. Mol. Opt. Phys. 66, 508 (2017)
- 265 32. F. Jarai-Szabo and L. Nagy, Eur. Phys. J. D 69, 4 (2015)
- 266 33. D.V. Karlovets, G.L. Kotkin, and V.G. Serbo, Phys. Rev. A 92, 052703 (2015)
- 267 34. L. Sarkadi and R. Barrachina, Phys. Rev. A 93, 032702 (2016)

- 268 35. I. Fabre, F. Navarrete, L. Sarkadi, and R.O. Barrachina, Eur. J. Phys. 39, 015401 (2018)
- 269 36. L. Gulyás, S. Egri, and A. Igarashi, Phys. Rev. A 99, 032704 (2019)
- 270 37. W.C. Keever and E. Everhart, Phys. Rev. 150, 43 (1966)
- 271 38. R. Schuch, E. Justiniano, H. Vogt, G. Deco, and N. Grün, J. Phys. B 24, L133 (1991)
- 272 39. R. Dörner, V. Mergel, L. Spielberger, O. Jagutzki, J. Ullrich, and H. Schmidt-Böcking, Phys. Rev. A 57, 312 (1998)
- 274 40. M. Schulz, T. Vajnai, and J.A. Brand, Phys. Rev. A 75, 022717 (2007)
 - 41. S.W. Bross, S.M. Bonham, A.D. Gaus, J.L. Peacher, T. Vajnai, H. Schmidt-Böcking, and M. Schulz, Phys. Rev. A 50, 337 (1994).



276

277

© 2020 by the authors. Submitted for possible open access publication under the terms and conditions of the Creative Commons Attribution (CC BY) license (http://creativecommons.org/licenses/by/4.0/).